

## Selective Laser Melting of Aluminium Alloys

Nesma T. Aboulkhair\*, Nicola M. Everitt, Ian Maskery, Ian Ashcroft, Chris Tuck

Metal additive manufacturing (AM) processes, such as selective laser melting, enable powdered metals to be formed into arbitrary 3D shapes. For aluminium alloys, which are desirable in many high-value applications for their low density and good mechanical performance, selective laser melting is regarded as challenging due to the difficulties in laser melting aluminium powders. However, a number of studies in recent years have demonstrated successful aluminium processing, and have gone on to explore its potential for use in advanced, AM componentry. In addition to enabling the fabrication of highly complex structures, selective laser melting produces parts with characteristically fine microstructures that yield distinct mechanical properties. Research is rapidly progressing in this field, with promising results opening up a range of possible applications across scientific and industrial sectors. This paper reports on recent developments in this area of research as well as highlighting some key topics that require further attention

**Keywords:** Al; Metal; Powder Processing; Rapid Solidification, Fatigue.

### Introduction to selective laser melting

Many industrial sectors are now benefiting from the possibility of fabricating intricate structures using additive manufacturing (AM) technologies to achieve the objectives of light-weighting, increased functionality and part number reduction. They also have the potential to fulfil demands for reducing the cost and design-to-manufacture time through savings on raw materials and replacement of a series of production processes by a single step process<sup>1,2</sup>, hence reducing lead times in multi-process fabrication<sup>3-7</sup>. Selective laser melting (SLM) is from the family of powder bed AM techniques. SLM involves a series of steps, principally powder deposition and laser scanning<sup>8</sup>, conducted within an inert controlled-atmosphere chamber to avoid oxidation<sup>9</sup>. The parts are normally built on a

temperature-controlled build-plate which acts as a heat sink and aids in heat dissipation by lowering the thermal gradient <sup>10</sup>, avoiding part curling due to non-uniform thermal expansion <sup>11</sup>.

Modern AM dates back to the mid-1980s and expanded during the late 1980s and early 1990s principally as a method for manufacturing prototypes quickly <sup>12, 13</sup>. Only recently has AM been considered part of a new industrial revolution <sup>14</sup>. A description of the evolution of AM can be found in <sup>15</sup>. SLM is gaining wide popularity across industrial and scientific research sectors <sup>13, 16</sup> for applications in the aerospace, automotive, and biomedical fields <sup>17</sup>. Components are fabricated from loose powder with comparable physical shape and properties and often even superior to those conventionally-manufactured (CM) <sup>4, 18</sup>. Part of the interest in SLM is driven by raising the level of automation in the manufacturing sector along with the production rates <sup>19</sup>. As a powder-bed process, SLM offers the geometrical flexibility to fabricate parts <sup>20</sup> that in many cases cannot be manufactured using CM <sup>4, 14</sup>; such as the examples in Figure 1. SLM promotes the possibility of producing highly-customized products <sup>14</sup> in low-to-medium quantities <sup>18, 21</sup>. Another benefit is eco-design optimization where significant structural light-weighting is possible, with a typically 50% weight-reduction <sup>22</sup>. SLM is also a promising technique to manufacture functionally-graded multi-material parts <sup>5, 23, 24</sup>.

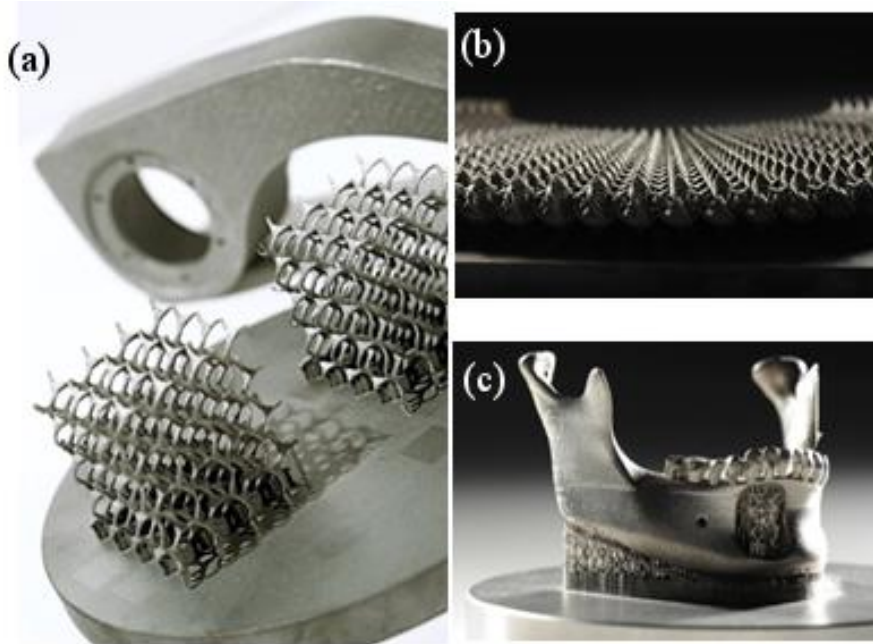


**Figure 1. Examples of complex structures manufactured using selective laser melting at the Centre for Additive Manufacturing (CfAM) laboratories at The University of Nottingham: (a) a stainless steel diamond lattice structure, (b) titanium designer necklace designed by Carrie Dickens, and (c) a jaw bone made from stainless steel.**

In SLM, a thin layer of feedstock powder is deposited by a wiper or roller mechanism. A laser then scans across the powder-bed line-by-line, melting the powder into cylindrical segments<sup>25</sup>; referred to as scan tracks (Figure 2a) or melt pools (Figure 2b). Scan tracks are similar to laser welds with the characteristic chevron pattern on top<sup>26</sup>. SLM samples are built up through metallurgical bonding of scan tracks overlapping in the horizontal and vertical directions (Figure 2c).

There are numerous useful reviews on metal AM, such as<sup>12, 28</sup>. The reader is directed to reference<sup>29</sup> for a generic review on AM processes. A review focusing on SLM of Al alloys<sup>30</sup> was published in 2015, however, a lot of progress has been made in this area of research after this date, which is included in this review. This review contributes to integrating the various aspects of the SLM process for Al alloys in the literature, which is beneficial to the academic community and various industrial sectors interested in SLM of Al alloys, such as the automotive and aerospace industries. A focus is the correlation between the process and the resultant microstructure, mainly governed by the mode of melting

and solidification behaviour, as well as the local and bulk mechanical behaviour of the material.

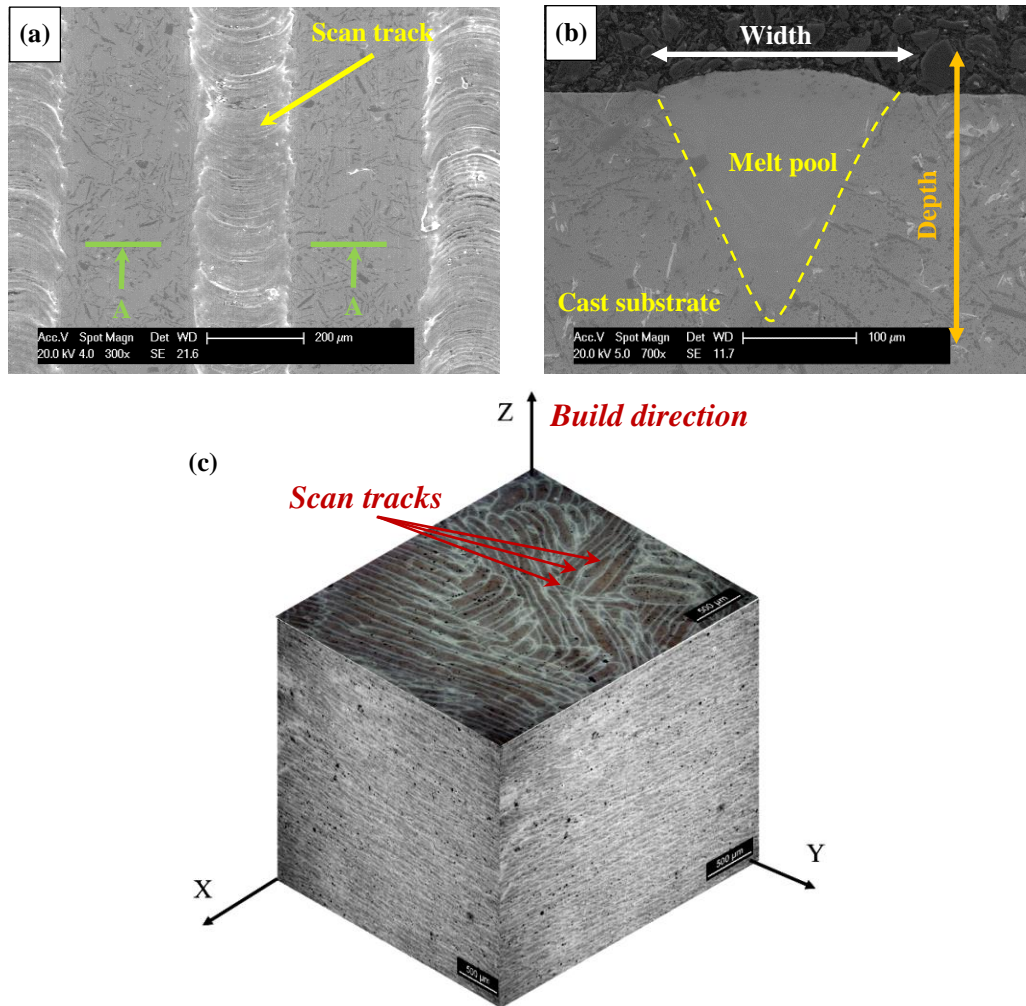


**Figure 1:** (a) Characteristic chevron pattern on top of an AlSi10Mg single track processed by SLM on an LM6 as-cast substrate and (b) cross-sectional view (A-A) of a single melt pool showing evidence of keyhole-mode melting, (c) isometric view for the orthogonal planes of a selectively laser melted cube from AlSi10Mg showing the overlapping tracks building up the part <sup>27</sup>.

### The suitability of aluminium alloys for SLM

A great deal of SLM research to date has focussed on the fabrication of steel and titanium components. Paving the way for SLM to become an attractive alternative to subtractive and forming CM requires widening the range of usable materials. Aluminium alloys are characterised by low density ( $2.7 \text{ gm/cm}^3$ ), high strength <sup>31</sup>, adequate hardenability <sup>32</sup>, good corrosion resistance <sup>33-35</sup>, and excellent

weld-ability<sup>32</sup>, making them suitable for use in a range of applications<sup>36</sup>, such as automotive, defence and aerospace equipment manufacturing, and machinery and tools production<sup>32, 33, 35</sup>. The possibility of manufacturing advanced lightweight Al parts using SLM opens up additional application opportunities and promotes the use of difficult-to-machine alloys. Examples of Al alloys examined for manufacture by SLM are shown in Table I, with AlSi10Mg having so far received the most attention. Further details on the classification of the Al alloys studied for SLM in the literature are available in<sup>37</sup>.

**Table I: Summary of works done in the field of SLM of Al alloys in the different focus areas listing the references.**

<b>Al alloys</b>	<b>Single tracks &amp; layers</b>	<b>Material qualification</b>	<b>Microstructure &amp; heat treatment</b>	<b>Mechanical properties</b>
<b>AlSi10Mg</b>	26, 47	38, 45	43, 48-52	20, 49, 52, 53
<b>Al-2618</b>	54	54		
<b>Al-2219</b>	54	54		
<b>Al-6061</b>		44		
<b>Al-7075</b>		46	46	46, 55
<b>A357</b>		56		56
<b>AlSi50</b>				57, 58
<b>AlSi12</b>		42, 59	60	42, 60
<b>Al-20Si-5Fe-3Cu-1Mg</b>			61	

### **The challenges of processing aluminium alloys by SLM**

As much as AM is finding its way into commercialization at a fast rate, not many materials are currently process-able<sup>13, 17</sup>. Compared to many other SLM candidate materials, Al alloys are challenging to process<sup>38</sup>. Aluminium powders are inherently light with poor flow-ability<sup>38, 39</sup>, high reflectivity in the typical SLM laser wavelength range, and high thermal conductivity<sup>34, 40</sup>. Laser

absorption of Al is poor<sup>40</sup> suggesting the need for high laser power to overcome the rapid heat dissipation<sup>35</sup>. They are highly susceptible to oxidation<sup>8, 33, 41, 42</sup>, which promotes porosity<sup>40, 43, 44</sup> alongside their low melt viscosity<sup>40</sup>. The major challenges addressed in the literature include minimizing porosity<sup>22, 38, 45</sup> and cracking<sup>46</sup>.

Numerous processing parameters are associated with SLM. These are known to affect the quality of the manufactured parts<sup>38</sup>, with ‘unoptimised’ parameters introducing defects, mainly porosity<sup>32, 62</sup>. The set of optimized parameters varies from one SLM machine to another and between materials. Therefore, “Material Development/Qualification Research”<sup>14, 19</sup> is crucial for the success of the process. The most frequently examined parameters<sup>8</sup> are the processing environment, powder properties, layer thickness, laser power, scan speed, hatch spacing, and scan strategy<sup>27</sup>.

SLM is conducted under inert atmosphere, typically argon<sup>38, 45</sup>. Wang et al.<sup>42</sup> reported the type of inert gas to have no effect on densification. However, Ferrar et al.<sup>4</sup> stated that the gas flow rate within the SLM chamber controls the amount of condensate and spatter removed during processing; these ejecta are generated by the laser-material interaction<sup>63, 64</sup>, with the amount of spatter related to the laser power and spot size<sup>14</sup>. Their structure and chemical composition were shown by Simonelli et al.<sup>64</sup> to be different from the feedstock powder. Inefficient removal of the spatter might lead to its entrapment as inclusions in the final parts, as has been observed by Aboulkhair et al.<sup>53</sup>, affecting final part densities.

There are some prerequisite powder properties to accommodate the successive deposition of uniform powder layers<sup>5, 38</sup>. Powder of a particular alloy can have different properties depending on the method of its manufacture and its processing history. Low porosity, higher quality parts are generally achieved when using powders complying with the process requirements<sup>39</sup>. This involves having spherical morphology, good flow-ability and packing density, minimal gas pores, and Gaussian particle size distribution. The flow-ability and apparent density of powders are improved by having particles of a spherical morphology<sup>6</sup> with a uniform Gaussian size distribution. The presence of gas phases in the

starting powder significantly suppresses densification<sup>65, 66</sup>. Pre-heating the powder is recommended to improve its laser absorptivity<sup>67</sup> and enhance densification<sup>59</sup>. Also, the use of the pre-sinter scan strategy<sup>38</sup> has been shown to significantly remedy powder-induced defects with powder that does not fully comply with the abovementioned requirements, yielding parts with a relative density that was comparable to those processed from higher quality powders<sup>39</sup>. It is important to consider the chemical composition of an alloy to be used in SLM since some chemical elements can make an alloy susceptible to cracking, as is common in difficult-to-weld alloys, such as Al-7075. Altering the chemical composition by adding elements that hinder cracking has been demonstrated to improve the process-ability, such as when amounts of Si were added to the Al-7075 to improve the fluidity, therefore eliminating the cracks<sup>46</sup>.

The consolidation of continuous single tracks can be used to determine a suitable range for laser power and scan speed for low porosity manufacture, as well as to define the layer thickness and hatch spacing through examination of the melt pool shape<sup>68</sup>. The basic requirements of single tracks can be found in<sup>26, 65</sup>. The stability of the melt pool is controlled by the processing parameters<sup>25, 54</sup>. The laser power and speed affect the width and depth of a scan track (Figure 2b), whereas its length is governed by the laser power and material's absorptivity<sup>62</sup>. Defects, such as satellites, balling, irregularities, and discontinuities<sup>26</sup>, can arise in Al tracks when the laser scan speed increases beyond a critical limit. Slower speeds are favoured because they increase the melt volume and enhance wettability rather than balling<sup>32</sup>. Aluminium's conductivity-reflectivity balance<sup>69</sup> results in keyhole-mode melting rather than conduction mode<sup>26</sup>, as demonstrated by the high depth-width ratio of the melt pool<sup>69</sup> in Figure 2b. The shape of the melt pool, whether spherical or conical, is an important factor when optimising the process parameters; the objective is to ensure sufficient overlap of the melt pools to create a consolidated defect-free layer through metallurgical bonding of adjacent scan tracks<sup>70</sup>. The conically-shaped melt pool in the case of Al requires the use of a narrow hatch spacing to create a consolidated layer, avoiding the formation of gaps towards the bottom through diminishing the intra-layer bonding

<sup>38</sup>. However, narrow hatch spacing results in slower rates of production, whilst larger hatch spacing impose a limitation on the maximum layer thickness <sup>70</sup>. Increasing the layer thickness promotes the formation of defects in tracks and layers <sup>26</sup>, hindering the deposition of uniform layers to build a multi-layered part. Furthermore, a large layer thickness results in reducing the re-melted depth <sup>26</sup>.

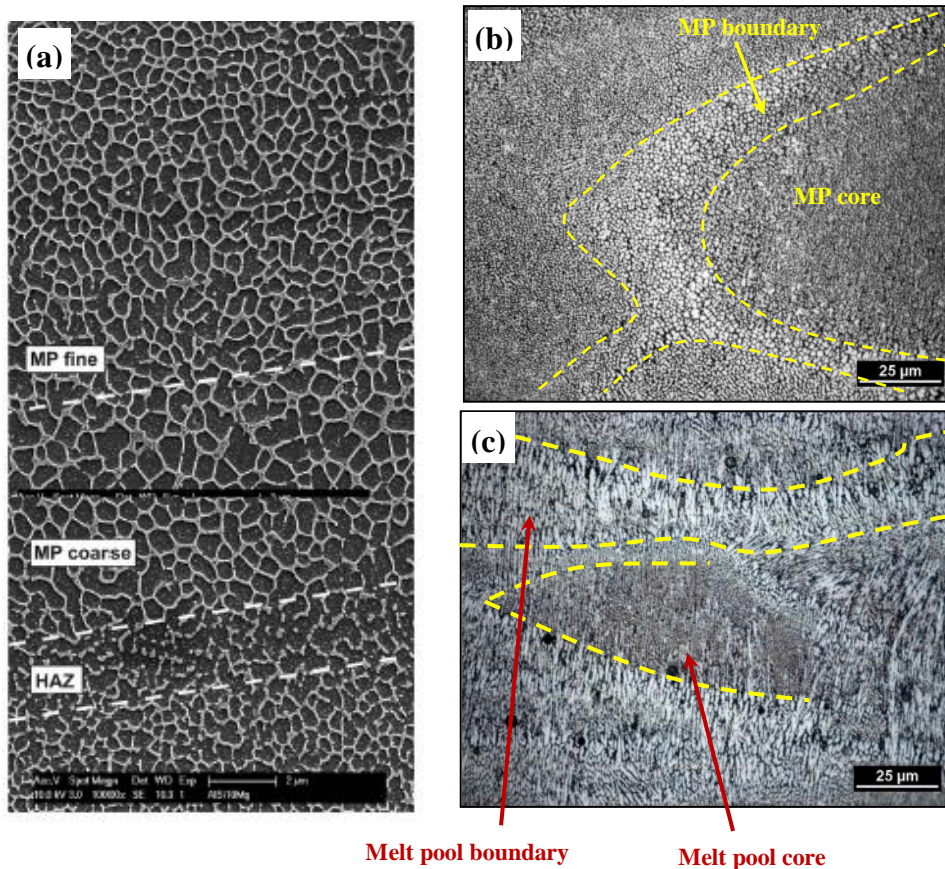
Two types of pores form during Al SLM, namely metallurgical and keyhole pores. The type of pore is scan speed dependent. A critical scan speed can be defined <sup>38</sup>, below which metallurgical (spherical) pores form and above which keyhole (irregular) pores are created. Altering the scan strategy has been employed with the aim of controlling the microstructure, minimizing the residual stresses <sup>43,71</sup>, and remedying defects, such as porosity <sup>38</sup>.

### **The metallurgy of SLM Al alloys**

A series of thermal processes during SLM <sup>12</sup> affect the resulting microstructure. Solidification occurs at a very fast rate producing a typically fine microstructure <sup>38</sup> and metastable phases <sup>72</sup>. The fine microstructure of SLM parts is in stark contrast to the generally coarse microstructures developed by CM processes <sup>32</sup>, and can be quite attractive for some applications. In addition, the material is re-melted more than once due to penetration of the laser beam and heat transfer. The microstructure within the melt pools of the scan tracks <sup>26</sup>, layers <sup>26,73</sup>, and multi-layered parts <sup>38,43,45,49</sup> has been repeatedly reported. Each melt pool is divided into three regions; the melt pool core, the melt pool boundary, and the heat affected zone (Figure 3a). The layer-based manufacturing approach results in microstructures that are non-homogeneous. Viewed perpendicularly to the build direction BD, the grains are equiaxed; being finer towards the melt pool core <sup>43</sup> (Figure 3b). Parallel to the BD, the grains at the melt pool boundaries are elongated, with finer equiaxed grains at the cores <sup>38,43</sup> (Figure 3c). Cellular-dendritic solidification produces fine equiaxed grains in the melt pool core due to proximity to the heat source and rapid solidification, with Si in the form of continuous segregations on the boundaries of  $\alpha$ -Al cells <sup>74</sup>, whereas grains at the melt pool boundary are columnar with inter-dendritic Si <sup>43</sup>. The dendritic growth indicates directional solidification along the thermal gradient, i.e. pointing



towards the moving heat source. Fast solidification also resulted in a fine and quite homogeneous dispersion of the alloying elements <sup>48</sup> (Figure 3e and f). Prashanth et al. <sup>74</sup> provided a clear explanation of the solidification process in SLM of Al-Si alloys attributing the formation of the cellular structure to the amount of undercooling. During solidification, Si is rejected into the liquid increasing the solute concentration. As per the Al-Si phase diagram, the solubility of Si in Al is reduced at lower temperatures but it can be extended by fast cooling. Therefore, the amount of Si rejected in the liquid during rapid cooling is reduced decreasing the solute concentration in the liquid as well as the undercooling. Rapid solidification changes the solute distribution drastically <sup>75</sup>. Thus a cellular structure is favoured in which  $\alpha$ -Al solidifies first in a cellular morphology leaving the remaining Si as segregations at the boundaries.



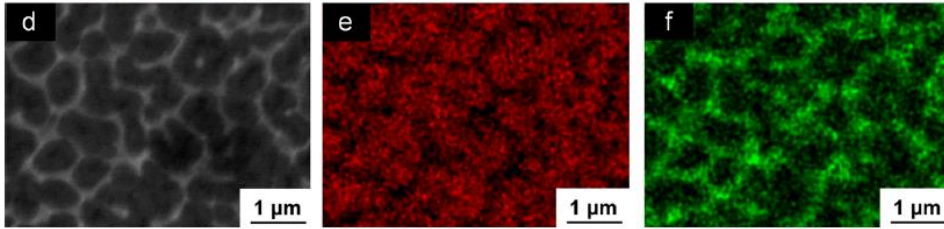


**Figure 2:** The microstructure of SLM AlSi10Mg showing (a) the three regions of microstructure within the melt pools divided into fine grains, coarse grains, and heat affected zones HAZ <sup>43</sup>, (b) equiaxed grains observed on the plane perpendicular to the build direction with coarser grains at the melt pool boundary, and (c) fine equiaxed grains at the melt pool core and coarser elongated grains at the melt pool boundary as seen in the plane parallel to the build direction <sup>48</sup>. (d) SEM image demonstrating a similar microstructure achieved for AlSi12 using SLM with (e and f) EDX maps showing the good dispersion of the alloying elements <sup>74</sup>.

During solidification, a fraction of the grains grow faster in preferred orientations, i.e. formation of a crystallographic texture develops in the material <sup>43</sup> due to the directional solidification and layer-by-layer fabrication (Figure 4a). Thijs et al. <sup>43</sup> reported the crystallographic texture of AlSi10Mg to change from a strong fibre texture to a weak cubic texture by changing the scan strategy (Figure 4b).

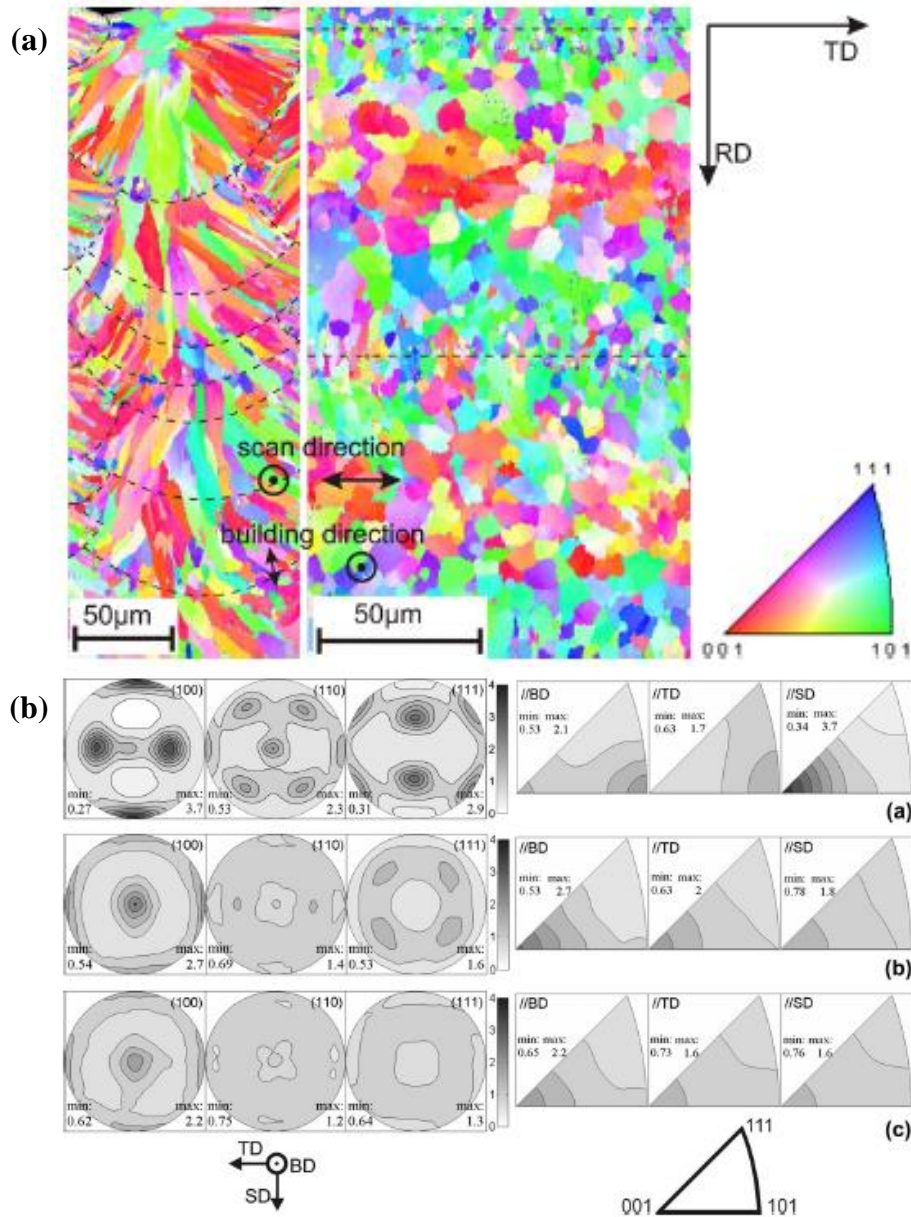


**Figure 3: (a) EBSD orientation maps for SLM AISi10Mg samples processed using the meander scan strategy and (b) the effect of changing the scan strategy on the crystallographic texture of the SLM AISi10Mg material <sup>43</sup>.**

The response of SLM Al to various post-manufacture heat treatments has been investigated in the literature. Annealing SLM Al-20%Si <sup>76</sup>, Al-12%Si <sup>74</sup>, and AISi10Mg <sup>50, 77</sup> led to Si diffusion to form particles (Figure 5a). As the treatment temperature or duration increased, the microstructure coarsened <sup>74</sup>. Heat treating AISi10Mg <sup>20, 48</sup> and 7075 <sup>46</sup> using solution heat treatment followed by artificial ageing (T6) also returned the same phase transformation (Figure 5b),



spherodisation (Figure 5c). Both heat treatment procedures dissolved the melt pools and dendritic structure. As the treatment duration increased, Si had a longer duration to diffuse and formed larger particles, decreasing their spatial density and increasing their size <sup>48</sup>.

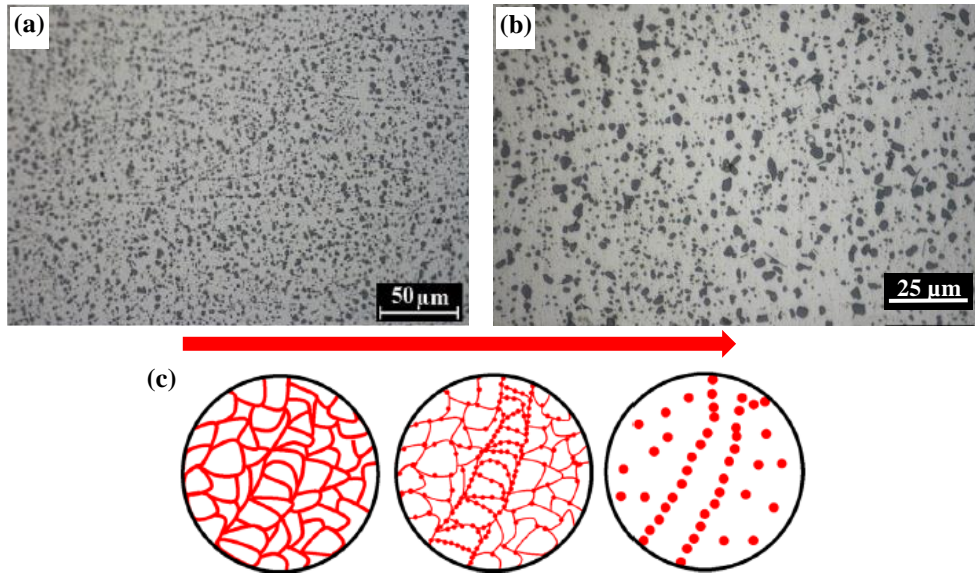


**Figure 4:** The microstructure of SLM AlSi10Mg after annealing heat treatment (a) <sup>50</sup> and solution heat treatment followed by artificial ageing (b) <sup>48</sup>. Both heat treatments promoted spherodisation phase transformation as illustrated in (c) <sup>74</sup>.

### The mechanical performance of SLM Al alloys

Material-laser interaction and rapid solidification due to high cooling rates ( $\sim 10^5$  K/s <sup>60</sup>) lead to microstructural modifications that can yield enhanced material properties <sup>36</sup> compared to CM material, e.g. cast material <sup>45</sup>. Mechanical characterization to assess the feasibility of using SLM for structural parts is ongoing, as demonstrated by the examples in Table II. Also, a summary of the tensile mechanical properties of SLM Al alloys reported in the literature can be found in <sup>37</sup>. Generally, SLM parts are characterized by high residual stresses arising from high energy density and rapid solidification <sup>78</sup>. High residual stresses in SLM AlSi12 ( $\sim 36$  MPa) were reduced by almost 90% by using a heated-build plate and post-process stress relief treatment <sup>79</sup>. The microstructure and porosity controlled by the process parameters influence the mechanical behaviour <sup>20</sup>. The

fine microstructure and good distribution of alloying elements (at the scale of several tens of microns) in SLM yield uniform local mechanical properties across the melt pools<sup>49</sup>. The global mechanical properties of SLM materials are comparable to those of their conventionally processed counterparts. Mechanical anisotropy is affected by the material's crystallographic texture<sup>80, 81</sup>, which is attributed to the process parameters<sup>43, 80</sup>. The layer-by-layer fashion in which the parts are built in SLM results in a number of factors leading to anisotropy<sup>82</sup>. These are: (1) the shape and size of voids, (2) the grain orientation and crystallographic texture with respect to the build orientation, and (3) the regions of interface between scan tracks and layers. When anisotropy is observed, better properties are generally seen along axes perpendicular to the BD<sup>20, 22, 80</sup>, with the density of dislocations being dependent on the BD<sup>81</sup>. However in some cases, no significant BD effect was observed<sup>20, 45</sup>.

**Table II: A list of the studies in the literature that investigated the various mechanical properties of SLM Al alloys.**

	AlSi10Mg	AlSi12	AlSi50	A357	Al-7075	Al-2xxx
<b>Nano-hardness</b>	26, 47, 49, 73					
<b>Micro-hardness</b>	22, 48, 80, 83		57		46	83
<b>Tensile behaviour</b>	22, 45, 49, 52, 77, 80, 84	42, 74, 79, 85, 86		56	55	
<b>Compressive behaviour</b>	49				46	
<b>Fatigue performance</b>	20, 53, 87, 88	60, 79, 86			55	
<b>Fracture toughness</b>		60				
<b>Creep resistance</b>	45					
<b>Impact resistance</b>	80					
<b>Wear behaviour</b>			57, 58			

Although several studies reported high tensile strengths for SLM parts compared with CM, this often comes at the expenses of low ductility. However, heat treatments such as annealing<sup>76</sup> and T6 procedures<sup>49</sup> can recover some of the

ductility without significantly reducing strength, providing a good compromise for applications which require both properties. The compromise between the SLM material's strength and ductility that can be achieved via heat treatment is appealing for numerous applications when considering the material's comparatively low density. A T6 heat treatment has been shown to soften SLM AlSi10Mg<sup>48</sup> and 7075<sup>46</sup>. The strengthening factors in the as-built and heat-treated materials were similar except for the grain size refinement factor in the former being replaced by the strengthening effect of dispersoids (Orowan) in the latter. The higher hardness in the SLM material indicates that the grain size refinement effect outweighed the dispersoid effect in this case.

The presence of un-bonded powder inside SLM parts was reported for AlSi10Mg<sup>38,45</sup>, 6061<sup>44</sup>, and 7075<sup>55</sup>. Although these regions are relatively small, i.e. they will not significantly reduce the load bearing area under tension<sup>45</sup>, they might be influential to fatigue. Defects in SLM parts act as stress concentrations, depressing fatigue life due to crack nucleation and growth<sup>20,78,89-91</sup>. SLM Al has shown good performance under cyclic loading<sup>20,53</sup>. The potential effect of machining to improve the fatigue performance was emphasised in some studies in the literature<sup>12</sup>, however, Aboulkhair et al.<sup>53</sup> provided evidence that machining may not improve the fatigue performance but rather increases the scatter in lifetime data. Heat treatment has been shown to considerably improve the fatigue performance<sup>20,53</sup> due to the transformation of Si dendrites to spheroids that hinder crack initiation and propagation<sup>20,53</sup>. The optimum fatigue life can be achieved by a combination of heat treatment and surface machining. The enhancement in fatigue life via heat treatment was attributed to the induced ductility and relaxation of residual stresses. Failure under tensile and cyclic loading always originated at sub-surface defects and propagated along the melt pool boundaries, this being the weaker region since it is Al-rich.

### **The future**

Despite the significant amount of work that has been done in the field of SLM of aluminium alloys, there are still areas that require the attention of the research and development community for a more mature impact on the industrial

sector. This section will highlight some of these areas, demonstrating their importance.

SLM commonly uses readily available pre-alloyed metal powder. The development of new SLM tailored powder mixtures has strong potential. Blending metal powders with different properties is a promising route. This could be in the form of altering the composition of pre-alloyed powder through adding modifiers or designing new alloys as in the case of SCALMALLOY®<sup>92</sup>. Coating Al or mixing it with elements that would enhance its absorptivity or surface tension could be a means for better material process-ability. The laser surface alloying literature<sup>93-95</sup> is rich with examples for improving the laser absorptivity through suitable additives. Depositing Cu on Al particles yielded particles with intermediate absorptivity and reflectance compared to the original elements<sup>96</sup>. Sistiaga et al.<sup>46</sup> added Si to Al-7075 alloy to improve the fluidity of the alloy, reduce the thermal expansion, and decrease the solidification range; successfully hindering the cracking common in SLM of Al-7075, producing defect-free parts. Vora et al.<sup>97</sup> compared processing pre-alloyed AlSi12 powder to blended Al and Si powder to the same composition demonstrating lower residual stressed when using blended powders. A means for mixing powders without just blending is satelliting<sup>98,99</sup> which is yet to be applied in SLM. Despite the potential in this approach, it is worth investigating the practicality of recycling the blended powders.

Several studies have stated the importance of using metal powders that have properties suitable for SLM. Standardizing properties of powders to be used for SLM is essential to cope with the process needs through producing powder with specifications meeting the process requirements. One of the appealing features in SLM is the ability to recycle the leftover powder. However, the literature on Al alloys lacks information on the threshold limit for powder recycling after which the quality of the produced parts and their mechanical performance is compromised. There are several studies on the powder recycling for other metal powders used in SLM<sup>100,101</sup> but the findings cannot be generalised for all materials. This is due to the presence of laser spatter in the left

over powder that has been found to have different properties from an alloy to another<sup>64</sup>. For example, the laser spatter from Ti-6Al-4V is not significantly different from the fresh powder, unlike AlSi10Mg spatter which has a distinct morphology and chemical composition.

As has been demonstrated in Table I, most of the research to date has been with Al-Si casting alloys with less consideration of the high strength alloys. This is due to the relative ease of processing the former compared to the latter, which in most cases not easily weldable, which is also indicative that they are not easily processed by SLM. The success of processing a hard-to-process alloy, such as Al-7075, through changing the chemical composition introduces the promising approach that is logical to adopt to widen the range of focus of aluminium alloys used in SLM. In addition to changing the chemical composition of alloys for better process-ability, chemical elements can be mixed into Al alloys with the aim of *in-situ* production of reinforced Al-based composites<sup>102, 103</sup>, such as AlSi10Mg and SiC with multiple reinforcements yielding superior mechanical properties<sup>104, 105</sup>, TiC reinforced Al-Si-Mg nano-composite from a mechanically-alloyed AlSi10Mg and TiC<sup>106</sup>, and TiC reinforced composite from mechanically-alloyed titanium, aluminium, and graphite<sup>107</sup>.

## References

1. M. Baumers, C. Tuck, R. Wildman, I. Ashcroft, E. Rosamond, R. Hague, 23<sup>rd</sup> Solid Freeform Fabr. Symp.(The University of Texas at Austin, Austin, TX, 2012), pp.932.
2. M. Baumers, C. Tuck, R. Wildman, I. Ashcroft, E. Rosamond, R. Hague, , J. Ind. Ecol. **17**, 418 (2013).
3. B. Zhang, H. Liao, C. Coddet, Mater. Des. **34**, 753 (2012).
4. B. Ferrar, L. Mullen, E. Jones, R. Stamp, C.J. Sutcliffe, J. Mater. Process. Tech. **212(2)**, 355 (2012).
5. I. Yadroitsev, P. Bertrand, I. Smurov, Appl. Surf. Sci. **253(19)**, 8064 (2007).
6. R. Li, Y. Shi, Z. Wang, L. Wang, J. Liu, W. Jiang, Appl. Surf. Sci. **256(13)** 4350 (2010).



7. M. Baumers, C. Tuck, R. Wildman, I. Ashcroft, R. Hague, J. Ind. Ecol. (2016), in press.
8. I. Gibson, D.W. Rosen, B. Stucker, Additive Manufacturing Technologies, Springer (2010).
9. L. Loeber, S. Biamino, U. Ackelid, S. Sabbadini, P. Epicoco, P. Fino, J. Eckert, 22<sup>nd</sup> Solid Freeform Fabr. Symp.(The University of Texas at Austin, Austin, TX, 2011), pp. 547.
10. K. Kempen, B. Vrancken, L. Thijs, S. Bols, J. Van Humbeeck, J.-P. Kruth, SFF **24**, (2013).
11. D. Buchbinder, W. Meiners, N. Pirch, K. Wissenbach, J. Schrage, J. Laser Appl. **26(1)**, 012004 (2014).
12. W.E. Frazier, J. Mater. Eng. Perform. **23(6)**, 12 (2014).
13. B.D. L., R.D. W., L. Ming, 3D Print. Addit. Manuf. **1(1)**, 4 (2014).
14. V. Matilainen, H. Piili, A. Salminen, T. Syvänen, O. Nyrhilä, Phys. Procedia **56(0)**, 317 (2014).
15. D.L. Bourell, J. Joseph J Beaman, M.C. Leu, D.W. Rosen, US – TURKEY Workshop On Rapid Technologies (2009).
16. D.C. Hofmann, S. Roberts, R. Otis, J. Kolodziejska, R.P. Dillon, J.O. Suh, A.A. Shapiro, Z.K. Liu, J.P. Borgonia, Sci. Rep. **4**, 5357 (2014).
17. N. Guo, M.C. Leu, Front.Mech. Eng. **8(3)** 215 (2013).
18. S. Leuders, M. Thöne, A. Riemer, T. Niendorf, T. Tröster, H.A. Richard, H.J. Maier, Int. J. Fatigue **48(0)**, 300 (2013).
19. H. Schleifenbaum, W. Meiners, K. Wissenbach, C. Hinke, J. Manuf. Sci. Technol. **2(3)**, 161 (2010).
20. E. Brandl, U. Heckenberger, V. Holzinger, D. Buchbinder, Mater. Des. **34(0)**, 159 (2012).
21. C.J. Tuck, R.J.M. Hague, M. Ruffo, M. Ransley, P. Adams, Int. J. Comput. Integ. M. **21(3)**, 245 (2008).
22. D. Buchbinder, H. Schleifenbaum, S. Heidrich, W. Meiners, J. Bültmann, Phys. Procedia **12, Part A(0)**, 271 (2011).
23. I. Yadroitsev, I. Smurov, Phys. Procedia **5, Part B(0)**, 551 (2010).

24. I. Maskery, N.T. Aboulkhair, A.O. Aremu, C.J. Tuck, I.A. Ashcroft, R.D. Wildman, R.J.M. Hague, *Mater. Sci. Eng. A* **670**, 264 (2016).
25. I. Yadroitsev, A. Gusarov, I. Yadroitsava, I. Smurov, *J. Mater. Process. Tech.* **210(12)**, 1624 (2010).
26. N.T. Aboulkhair, I. Maskery, C. Tuck, I. Ashcroft, N.M. Everitt, *J. Mater. Process. Tech.* **230**, 88 (2016).
27. N.T. Aboulkhair, Additive manufacture of an aluminium alloy: processing, microstructure, and mechanical properties, Department of Mechanical, Materials, and Manufacturing Engineering, University of Nottingham, UK, 2015.
28. E. Herderick, *Proceedings of MS&T 2011* (2011).
29. K.V. Wong, A. Hernandez, *ISRN Mech. Eng.* **2012**, 1 (2012).
30. E.O. Olakanmi, R.F. Cochrane, K.W. Dalgarno, *Prog. Mater. Sci.* **74(0)**, 401 (2015).
31. M. Tisza, *Physical metallurgy for engineers*, ASM International and Freund Publishing House Ltd.2002.
32. Y. Li, D. Gu, *Mater. Des.* **63(0)**, 856 (2014).
33. G.E. Totten, D.S. Mackenzie, *Handbook of Aluminum: Physical Metallurgy and Processes*, 1 ed., CRC press, New York, 2003.
34. I.J. Polmear, *Light alloys: metallurgy of the light metals*, 3rd edition ed.
35. W.H. Hosford, *Physical Metallurgy*, Second ed., CRC Press, United States of America, 2010.
36. S. Dadbakhsh, L. Hao, *J. Alloy. Compd.* **541(0)**, 328 (2012).
37. Y. Ding, J.A. Muñiz-Lerma, M. Trask, S. Chou, A. Walker, M. Brochu, *MRS Bulletin* **41(10)**,745 (2016).
38. N.T. Aboulkhair, N.M. Everitt, I. Ashcroft, C. Tuck, *Addit. Manuf.* **1-4(0)**, 77 (2014).
39. N.T. Aboulkhair, I. Maskery, I. Ashcroft, C. Tuck, N.M. Everitt, *Lasers in Manufacturing conference*, (Munich, Germany, 2015).
40. J.C. Ion, *Laser processing of engineering materials: Principles, Procedure and Industrial application*, El Sevier, United Kingdom, 2005.

41. Handbook of Aluminum: Volume 2: Alloy Production and Materials Manufacturing, 2003.
42. X.J. Wang, L.C. Zhang, M.H. Fang, T.B. Sercombe, Mater. Sci. Eng.A **597(0)**, 370 (2014).
43. L. Thijs, K. Kempen, J.-P. Kruth, J. Van Humbeeck, Acta Mater. **61(5)**, 1809 (2013).
44. E. Louvis, P. Fox, C.J. Sutcliffe, J. Mater. Process. Technol. **211(2)**, 275 (2011).
45. N. Read, W. Wang, K. Essa, M.M. Attallah, Mater. Des. **65(0)**, 417 (2015).
46. M.L. Montero Sistiaga, R. Mertens, B. Vrancken, X. Wang, B. Van Hooreweder, J.-P. Kruth, J. Van Humbeeck, J. Mater. Process. Technol. **238**, 437 (2016).
47. N.T. Aboulkhair, I. Maskery, C. Tuck, I. Ashcroft, N. Everitt, SPIE, 2015, pp. 965702-965702-7.
48. N.T. Aboulkhair, C. Tuck, I. Ashcroft, I. Maskery, N.M. Everitt, Metall. Mater. Trans. A **46A(8)**, 3337 (2015).
49. N.T. Aboulkhair, I. Maskery, C. Tuck, I. Ashcroft, N.M. Everitt, Mater. Sci. Eng. A **667**, 139 (2016).
50. I. Maskery, N.T. Aboulkhair, M.R. Corfield, C. Tuck, A.T. Clare, R.K. Leach, R.D. Wildman, I.A. Ashcroft, R.J.M. Hague, Mater. Charact. **111**, 193 (2016).
51. J. Wu, X.Q. Wang, W. Wang, M.M. Attallah, M.H. Loretto, Acta Mater. **117**, 311 (2016).
52. I. Rosenthal, A. Stern, N. Frage, Metallography, Microstructure, and Analysis **3(6)**, 448 (2014).
53. N.T. Aboulkhair, I. Maskery, C. Tuck, I. Ashcroft, N.M. Everitt, Mater. Des. **104**, 174 (2016).
54. B. Ahuja, M. Karg, K.Y. Nagulin, M. Schmidt, Phys. Procedia **56(0)**, 135 (2014).
55. W. Reschetnik, J.P. Brüggemann, M.E. Aydinöz, O. Grydin, K.P. Hoyer, G. Kullmer, H.A. Richard, Procedia Structural Integrity **2**, 3040 (2016).
56. H. Rao, S. Giet, K. Yang, X. Wu, C.H.J. Davies, Mater. Des. **109**, 334 (2016).

57. N. Kang, P. Coddet, C. Chen, Y. Wang, H. Liao, C. Coddet, *Mater. Des.* **99**, 120 (2016).
58. N. Kang, P. Coddet, H. Liao, T. Baur, C. Coddet, *Appl. Surf. Sci.* **378**, 142 (2016).
59. X.P. Li, K.M. O'Donnell, T.B. Sercombe, *Addit. Manuf.* **10**, 10 (2016).
60. J. Suryawanshi, K.G. Prashanth, S. Scudino, J. Eckert, O. Prakash, U. Ramamurty, *Acta Mater.* **115**, 285 (2016).
61. P. Ma, Y. Jia, K.G. Prashanth, S. Scudino, Z. Yu, J. Eckert, *J. Alloy. Compd.* **657**, 430 (2016).
62. C. Kamath, B. El-dasher, G.F. Gallegos, W.E. King, A. Sisto, Livermore, California. UNT Digital Library.  
<http://digital.library.unt.edu/ark:/67531/metadc872227/>. Accessed October 26, 2016.
63. C. Tuck, I. Maskery, M. Simonelli, N. Aboulkhair, I. Ashcroft, N. Everitt, R. Wildman, R. Hague, TMS Annual meeting and exhibition, 2015.
64. M. Simonelli, C. Tuck, N.T. Aboulkhair, I. Maskery, I. Ashcroft, R.D. Wildman, R. Hague, *Metall. Mater. Trans. A* **46A(9)**, 3842 (2015).
65. K. Kempen, L. Thijs, E. Yasa, M. Badrossamay, W. Verheecke, J.-P. Kruth, 22<sup>nd</sup> Solid Freeform Fabr. Symp. (The University of Texas at Austin, Austin, TX, 2011), pp. 484-495.
66. D. Dai, D. Gu, *Mater. Des.* **55(0)**, 482 (2014).
67. I. Yadroitsev, P. Krakhmalev, I. Yadroitsava, S. Johansson, I. Smurov, *J. Mater. Process. Technol.* **213(4)**, 606 (2013).
68. Y. Pupo, J. Delgado, L. Serenó, J. Ciurana, *Procedia Eng.* **63(0)**, 370 (2013).
69. W.E. King, H.D. Barth, V.M. Castillo, G.F. Gallegos, J.W. Gibbs, D.E. Hahn, C. Kamath, A.M. Rubenchik, *J. Mater. Process. Technol.* **214(12)**, 2915 (2014).
70. X. Su, Y. Yang, *J. Mater. Process. Technol.* **212(10)**, 2074 (2012).
71. M. Simonelli, Y.Y. Tse, C. Tuck, *Metall. Mater. Trans.* **A45(6)**, 2863 (2014).
72. Aluminum: properties and physical metallurgy, American society for metals, Ohio, 1984.

73. Nicola M. Everitt, Nesma T. Aboulkhair, Ian Maskery, Chris Tuck, I. Ashcroft, *Adv. Mater. Letters* **7(1)**, 13 (2016).
74. K.G. Prashanth, S. Scudino, H.J. Klauss, K.B. Surreddi, L. Löber, Z. Wang, A.K. Chaubey, U. Kühn, J. Eckert, *Mater. Sci. Eng. A* **590(0)**, 153 (2014).
75. W. Kurz, R. Trivedi, *Metall. Mater. Trans.* **A22(12)**, 3051 (1991).
76. P. Ma, K.G. Prashanth, S. Scudino, Y.D. Jia, H.W. Wang, C.M. Zou, Z.J. Wei, J. Eckert, *Metals* **4(1)**, 28 (2014).
77. W. Li, S. Li, J. Liu, A. Zhang, Y. Zhou, Q. Wei, C. Yan, Y. Shi, *Mater. Sci. Eng. A* **663**, 116 (2016).
78. P. Edwards, M. Ramulu, *Mater. Sci. Eng. A* **598(0)**, 327 (2014).
79. S. Siddique, M. Imran, E. Wycisk, C. Emmelmann, F. Walther, , *J. Mater. Process. Technol.* **221(0)**, 205 (2015).
80. K. Kempen, L. Thijs, J. Van Humbeeck, J.P. Kruth, *Phys. Procedia* **39(0)**, 439 (2012).
81. P. Kanagarajah, F. Brenne, T. Niendorf, H.J. Maier, *Mater. Sci. Eng. A* **588(0)**, 188 (2013).
82. D. Buchbinder, W.Meiners, K. Wissenbach, R. Poprawe, *J. Laser Appl.* **27**, S29205 (2015).
83. K. Bartkowiak, S. Ullrich, T. Frick, M. Schmidt, *Phys. Procedia* **12, Part A(0)**, 393 (2011).
84. U. Tradowsky, J. White, R.M. Ward, N. Read, W. Reimers, M.M. Attallah, *Mater. Des.* **105**, 212 (2016).
85. K.G. Prashanth, R. Damodaram, S. Scudino, Z. Wang, K. Prasad Rao, J. Eckert, *Mater. Des.* **57(0)**, 632 (2014).
86. S. Siddique, M. Imran, F. Walther, *Int. J. Fatigue*, in press.
87. I. Maskery, N.T. Aboulkhair, C. Tuck, R.D. Wildman, I.A. Ashcroft, N.M. Everitt, R.J.M. Hague, *26<sup>th</sup> Solid Freeform Fabr. Symp. (The University of Texas at Austin, Austin, TX, 2015)*, pp. 1017-1025.
88. M. Tang, P. Chris Pistorius, *Int. J. Fatigue*, in press.
89. R. González, A. González, J. Talamantes-Silva, S. Valtierra, R.D. Mercado-Solís, N.F. Garza-Montes-de-Oca, R. Colás, *Int. J. Fatigue* **54(0)**, 118 (2013).

90. Eliahu Zahavi, V. Torbilo, Fatigue design - Life expectancy of machine parts, CRC Press 1996.
91. S. Suresh, Fatigue of materials, 2nd ed., Cambridge University Press 1998.
92. Airbus-Group, SCALMALLOY®RP Auminum-Magnesium-Scandium alloy powder. <<http://www.technology-licensing.com/etl/int/en/What-we-offer/Technologies-for-licensing/Metallics-and-related-manufacturing-technologies/Scalmalloy-RP.html>>, (accessed 19 Novermber 2014.2014).
93. R.S. Razavi, G.R. Gordani, Laser Surface Treatments of Aluminum Alloys, in: P.Z. Ahmed (Ed.), Recent Trends in Processing and Degradation of Aluminium Alloys, InTech, 2011.
94. D.S. Gnanamuthu, Laser Surface Treatment, Optic. Eng. **19(5)**, 195783 (1980).
95. S. Tomida, K. Nakata, S. Saji, T. Kubo, Surf. Coat. Technol. **142–144**, 585 (2001).
96. M. Sachs, O. Hentschel, J. Schmidt, M. Karg, M. Schmidt, K.-E. Wirth, Phys. Procedia **56(0)**, 125 (2014).
97. P. Vora, K. Mumtaz, I. Todd, N. Hopkinson, Addit. Manuf. **7**, 12 (2015).
98. A. Clare, A. Kennedy, Additive manufacturing, Patent number US 20160279703 A1, The University of Nottingham, United Kingdom, 2016.
99. A.N.D. Gasper, S. Catchpole-Smith, A.T. Clare, J. Mater. Process. Technol. **239**, 230 (2017).
100. L.C. Ardila, F. Garciandia, J.B. González-Díaz, P. Álvarez, A. Echeverria, M.M. Petite, R. Deffley, J. Ochoa, Phys. Procedia **56(0)**, 99 (2014).
101. V. Seyda, N. Kaufmann, C. Emmelmann, Phys. Procedia **39**, 425 (2012).
102. S. Dadbakhsh, L. Hao, The Scientific World Journal **2014**, 106129 (2014).
103. S. Dadbakhsh, L. Hao, P.G.E. Jerrard, D.Z. Zhang, Powder Technol. **231(0)**, 112 (2012).
104. D. Gu, F. Chang, D. Dai, J. Manuf. Sci. Eng. **137 (2)**, 021010 (2014).
105. D. Gu, H. Wang, F. Chang, D. Dai, P. Yuan, Y.-C. Hagedorn, W. Meiners, Phys. Procedia **56(0)**, 108 (2014).

106. D.D. Gu, H.Q. Wang, D.H. Dai, P.P. Yuan, W. Meiners, R. Poprawe, *Scripta Mater.* **96(0)**, 25 (2015).

107. D. Gu, Z. Wang, Y. Shen, Q. Li, Y. Li, *Appl. Surf. Sci.* **255(22)**, 9230 (2009).

### **Author biographies**

#### **Nesma T. Aboulkhair**

Additive Manufacturing and 3D Printing Research Group

Faculty of Engineering, University of Nottingham

Nottingham, NG7 2RD, United Kingdom.

*Telephone:* +447539519516

*E-mail address:* nesma.aboulkhair@nottingham.ac.uk

Nesma is a research fellow in the centre for AM. She holds a BSc in Mechanical Engineering from Cairo University, MSc in Mechanical Engineering from the American University in Cairo, and PhD in Materials Engineering and Materials Design from the University of Nottingham. Nesma was awarded numerous fellowships and prizes throughout her studies. Her current research spans across various AM processes. She has a broad experience in metal additive manufacturing and strong knowledge in metallurgy and materials characterisation.

#### **Nicola M. Everitt**

Bioengineering Research Group

Faculty of Engineering, University of Nottingham

Nottingham, NG7 2RD, United Kingdom.

*E-mail address:* nicola.everitt@nottingham.ac.uk

Dr. Nicola Everitt (B.Sc. (Hons) in Materials Science and D.Phil. (Oxon)) has been an Associate Professor at the University of Nottingham in the Department of Mechanical, Materials and Manufacturing Engineering since 2001. Nicola has particular interest and expertise in micro- and nano-indentation testing, and dynamic materials analysis i.e. the behaviour of materials at different rates of loading or strain at different temperatures. This work is very relevant to understanding the behaviour of 3D printed structures.

**Ian Maskery**

Additive Manufacturing and 3D Printing Research Group  
Faculty of Engineering, University of Nottingham  
Nottingham, NG7 2RD, United Kingdom.

*E-mail address:* ian.maskery@nottingham.ac.uk

Ian Maskery attended the University of York for four years until 2009, obtaining an MPhys degree with first class honours. He obtained his PhD in Physics from the University of Warwick in 2013. Since then, Ian has been a postdoctoral researcher at the University of Nottingham, where he has investigated the properties of materials made by selective laser melting. Ian also investigates the use of lightweight cellular structures in additive manufacturing, examining relationships between their design, manufacture and mechanical performance.

**Ian Ashcroft**

Additive Manufacturing and 3D Printing Research Group  
Faculty of Engineering, University of Nottingham  
Nottingham, NG7 2RD, United Kingdom.

*E-mail address:* ian.ashcroft@nottingham.ac.uk

Ian Ashcroft is Professor of Solid Mechanics at the University of Nottingham. His expertise is in both experimental and computational mechanics with particular interest in the effects of complex loading and environment on materials and structures. Recently, he has focussed his research into the application of solid mechanics to additive manufacturing, particularly in developing multi-physics modelling techniques for AM processes and the post processing performance of parts and the development of design and optimisation techniques for various AM technologies.

**Chris Tuck**

Additive Manufacturing and 3D Printing Research Group  
Faculty of Engineering, University of Nottingham  
Nottingham, NG7 2RD, United Kingdom.

*E-mail address:* christopher.tuck@nottingham.ac.uk



Prof Chris is an expert in Additive Manufacturing materials, process and applications. Holding a BEng (Hons) in Materials Science and Engineering from Brunel University and an EngD from Cranfield University. Currently running a number of projects around multi-material and multifunctional AM systems, and the development of metallic AM systems for use in industry. Chris is Director of the EPSRC Centre for Doctoral Training in AM. Chris is Co-Founder of the spin out company Added Scientific.